

The Shapes of Things to Come: Probability Density Quantiles

Robert G. Staudte

16 December, 2016

Abstract

For every discrete or continuous location-scale family having a square-integrable density, there is a unique continuous probability distribution on the unit interval that is determined by the density-quantile composition introduced by Parzen in 1979. These *probability* density quantiles (pdQs) only differ in *shape*, and can be usefully compared with the Hellinger distance or Kullback-Leibler divergences. Convergent empirical estimates of these pdQs are provided, which leads to a robust global fitting procedure of shape families to data. Asymmetry can be measured in terms of distance or divergence of pdQs from the symmetric class. Further, a precise classification of shapes by tail behavior can be defined simply in terms of pdQ boundary derivatives.

Keywords: *asymmetry; Hellinger metric; quantile density; Kullback-Leibler divergence; Lagrange multipliers; tail-weight*

1 Introduction

The study of shapes of probability distributions is simplified by viewing them through the revealing composition of density with quantile function. Following normalization, the resulting functions are not only location-scale free, but densities of absolutely continuous distributions having the same support. This microcosm of *probability density quantiles* carries essential information regarding shapes and allows for simpler classification by asymmetry and tail weights. It also leads to an alternative and effective method for fitting shape families to data.

1.1 Background and summary

In the seminal work Parzen (1979) proposed that traditional statistical inference be connected to exploratory data analysis through transformations from standard continuous models (normal, exponential) to the realm of density quantile functions. If the standard models were rejected by goodness-of-fit tests, the next step was nonparametric modeling, with the emphasis on what could be gleaned from sample quantile functions and time series methods. The quantile approach to data analysis was earlier championed by Tukey (1962, 1965, 1977), who also provided insightful commentary into Parzen's proposals. Further work on quantile-based data modeling can be found in Gilchrist (2000), Parzen (2004), while Jones (1992) investigates estimation of density quantile functions and their reciprocals.

Here we study the classification of shapes for *probability* density quantiles. While this class is limited by the requirement of square-integrability of the density function, it is rich enough to warrant investigation because the transformation from density to the normalized composition of density function with quantile function allows for comparison of shapes of both discrete

and continuous models using the Hellinger metric and Kullback-Leibler divergences—with non-trivial and informative results.

In this Section we formally introduce pdQs for discrete and continuous distributions and provide numerous examples, including moments in the continuous case. Given data, in Section 2 we describe methods for estimating the pdQ's of discrete and continuous distributions, respectively. These are employed in Section 3 where global robust fitting of shape parameter families to data based on the Hellinger distance from the empirical pdQ are implemented.

In Section 4 we measure asymmetry of the pdQ in terms of its distance or divergence from the class of symmetric distributions; and, we show they can be predicted by the skewness coefficient of the pdQ. In Section 5 we introduce a simple but absolute tail-weight classification in terms of the boundary derivatives of the pdQs. Further challenges are posed in Section 6.

1.2 Definitions and properties

Let \mathcal{F} be the class of all right-continuous cumulative distribution functions (cdf s) on the real line. For each $F \in \mathcal{F}$ define the associated left-continuous *quantile function* of F by $Q(u) \equiv \inf\{x : F(x) \geq u\}$, for $0 < u < 1$. When the random variable X has cdf F , write $X \sim F$. In particular, let $U \sim \mathcal{U}$ where U has the uniform distribution on $[0,1]$. Let $\mathcal{F}' = \{F \in \mathcal{F} : f = F' \text{ exists and is positive}\}$. For each $F \in \mathcal{F}'$ we follow Parzen (1979) and define the *quantile density function* $q(u) = Q'(u) = 1/f(Q(u))$, Tukey (1965) also recognized its importance and called it the *sparsity index*. Its reciprocal $fQ(u) \equiv f(Q(u))$ is called the *density quantile function*. In order to convert density quantiles into *probability densities* we need to compute $\kappa \equiv E[fQ(U)] = \int f^2(x) dx$.

Definition 1 For $F \in \mathcal{F}'$, assume $\kappa = E[fQ(U)]$ is finite; that is, f is square integrable. Then define the probability density quantile or pdQ of F by $f^*(u) = fQ(u)/\kappa$, $0 < u < 1$. Let $\mathcal{F}^{*} \subset \mathcal{F}'$ denote the class of all such F .

Not all densities are square integrable, and for such densities a pdQ does not exist. Examples are the Chi-squared densities with degrees of freedom $\nu \leq 1$. Others are the Beta(a, b) densities with $a \leq 1/2$ or $b \leq 1/2$. Unless otherwise noted we follow standard definitions for distributions as described in Johnson *et al.* (1994, 1995).

An important property of pdQs is that they are location-scale invariant. For if $F_{a,b}(\cdot) \equiv F((\cdot - a)/b)$ for arbitrary a and $b > 0$ defines the location-scale family generated by $F = F_{0,1} \in \mathcal{F}$, then the quantile function for $F_{a,b}$ is $Q_{a,b}(u) = a + bQ(u)$. Further, if $F \in \mathcal{F}'$ the quantile density is $q_{a,b}(u) = bq(u)$; thus the quantile density is location-invariant and scale equivariant. Clearly $f_{a,b}^*$ is also scale invariant, and one can write $f_{a,b}^* = f_{0,1}^* = f^*$. Thus when comparing the graphs of different f^* s, we are comparing only their *shapes*.

Conversely, given an $f^* \in \mathcal{F}^{*}$, one can identify the family $\{F_{a,b} : a, b > 0\}$. For if it is known that f^* has the form $f^* = (fQ)/\kappa$, for some unknown F with associated density $f = F'$, inverse Q , quantile density $q = 1/(fQ)$ and $\kappa = E[fQ(U)]$, then one can reconstruct $Q(u) = \int_0^u q(t) dt + c = \kappa \int_0^u \{f^*(t)\}^{-1} dt + c$; thus Q is determined up to location and scale, as is F . An open question is whether, given an arbitrary continuous distribution with probability density g on $(0, 1)$, does there exist an $F \in \mathcal{F}'$ such that $g = f^*$?

Another property of pdQs is that they ignore flat spots in F . For example, the pdQ f_{gap}^* of $f_{\text{gap}}(x) = (e^x/2) I_{(-\infty, 0]}(x) + I_{[1/2, 1]}(x)$ equals that of $f(x) = (e^x/2) I_{(-\infty, 0]}(x) + I_{[0, 1/2]}(x)$. Thus it is only the shape of the distribution on its *support* that is captured by the pdQ.

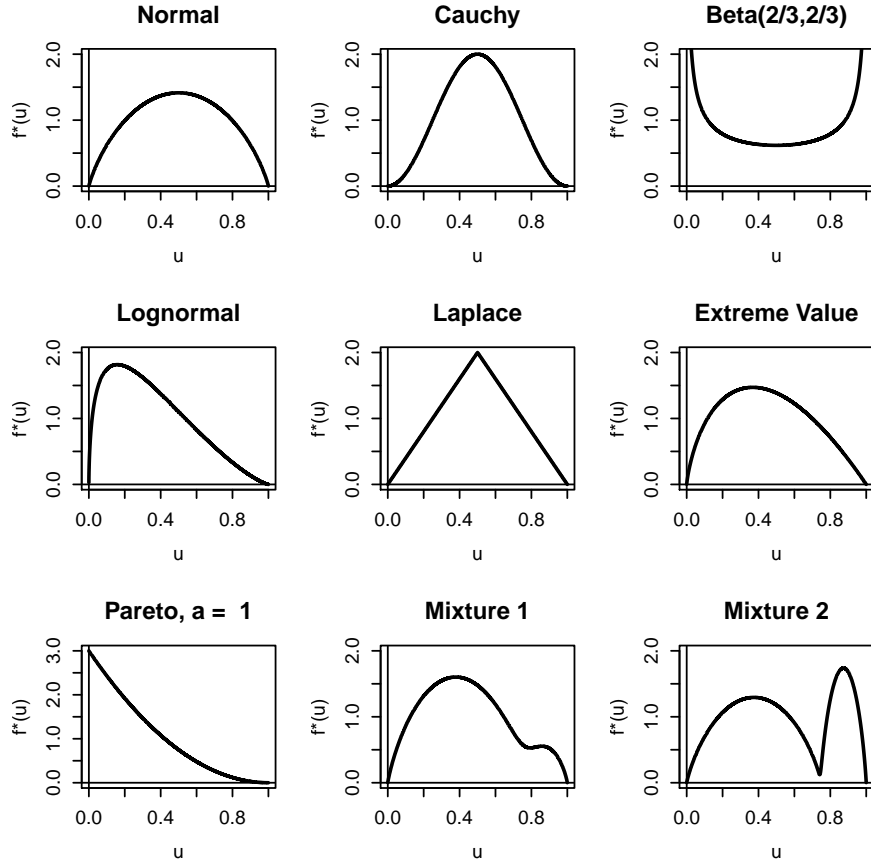


Figure 1: $pdQs$ of some standard continuous distributions, plus two mixtures of normal distributions. Details are given in Section 1.3.

1.3 Examples of continuous $pdQs$

Many of the $pdQs$ $f^*(u) = fQ(u)/\kappa$ discussed in this section are merely normalized versions of density quantiles fQ described in Parzen (1979); some formulae for $f^*(u)$ are given in Table 1.

For the normal distribution Φ with density φ , we write $z_u = \Phi^{-1}(u)$ and then it has $\varphi^*(u) = 2\sqrt{\pi}\varphi(z_u)$. Its graph is shown in the upper left plot of Figure 1. It is quite close to that of a quadratic function which is symmetric about $1/2$ and passes through $(0,0)$ and $(1/2, \sqrt{2})$, and not unlike the exact quadratic $f^*(u) = 6u(1-u)$ corresponding to the logistic distribution (not shown). The U-shaped Beta(2/3,2/3) distribution retains its U-shape, and the bell-shaped Cauchy retains a bell-shape after transformation to the quantile scale. The Laplace (double-exponential) family transforms to the symmetric triangular distribution.

The Tukey(λ) family is defined by its quantile function $Q_\lambda(u) = \{u^\lambda - (1-u)^\lambda\}/\lambda$ for $\lambda \neq 0$ and $Q_0(u) = \ln(u/(1-u))$, but in general no closed form expression is available for its density. For $\lambda > 0$ the density has finite support $[-1/\lambda, +1/\lambda]$, and otherwise has infinite support. It has pdQ $f_\lambda^*(u) = 1/\{Q'_\lambda(u)\kappa_\lambda\} = \{u^{\lambda-1} + (1-u)^{\lambda-1}\}^{-1}/\kappa_\lambda$. The constant κ_λ required to make $\int f_\lambda^*(u) = 1$ can be obtained by numerical integration but a good approximation is given by:

$$\kappa_\lambda \approx \begin{cases} \frac{3^\lambda}{6}, & \lambda \leq 1; \\ \frac{\lambda}{2}, & 1 \leq \lambda \leq 2; \\ \left(\frac{2}{\pi}\right)^{\lambda-2}, & 2 \leq \lambda \leq 6. \end{cases} \quad (1)$$

For $\lambda \leq 2$ the absolute error of this approximation is less than 0.005, and for $2 \leq \lambda \leq 6$ it is less 0.1. The absolute relative error of approximation is less than 0.06 for $-1 \leq \lambda \leq 6$.

Table 1: **Some continuous distributions F and their quantile functions and pdQs.** In general, we denote $x_u = Q(u) = F^{-1}(u)$, but for the normal $F = \Phi$ with density φ , we write $z_u = \Phi^{-1}(u)$. The power function distribution is also known as the Beta($b, 1$) family. For the Weibull(β) family, no simple approximation for κ_β is available. Similarly for the Tukey(λ) family, κ_λ is not available, but a simple approximation is given in Section 1.3.

	$F(x)$	$Q(u)$	$f^*(u)$
Power(b)	$x^b, 0 < x < 1$	$u^{1/b}$	$(2 - \frac{1}{b})u^{1-1/b}, b > 1/2$
Laplace	$e^x/2, x < 0$ $1 - e^{-x}/2, x \geq 0$	$\ln(2u), u \leq 0.5$ $-\ln(2(1-u)), u \geq 0.5$	$2 \min\{u, 1-u\}$
Logistic	$e^x(1+e^x)^{-1}$	$\ln(u/(1-u))$	$6u(1-u)$
Extreme Value	$e^{-e^{-x}}$	$-\ln(-\ln(u))$	$-4u \ln(u)$
Cauchy	$\frac{1}{\pi} \arctan(x) - \frac{1}{2}$	$\tan\{\pi(u-0.5)\}$	$2 \sin^2(\pi u)$
Tukey(λ)	—	$\lambda^{-1}\{u^\lambda - (1-u)^\lambda\}$	$\{\kappa_\lambda (u^{\lambda-1} + (1-u)^{\lambda-1})\}^{-1}$
Normal	$\Phi(x)$	z_u	$2\sqrt{\pi} \varphi(z_u)$
Lognormal	$\Phi(\ln(x)), x > 0$	e^{z_u}	$\frac{2\sqrt{\pi}}{e^{1/4}} \varphi(z_u) e^{-z_u}$
Type I Pareto(a)	$1 - x^{-a}, x > 1$	$(1-u)^{-1/a}$	$(2 + \frac{1}{a})(1-u)^{1+1/a}$
Exponential	$1 - e^{-x}, x > 0$	$-\ln(1-u)$	$2(1-u)$
Weibull(β)	$1 - e^{-x^\beta}, x > 0$	$\{-\ln(1-u)\}^{1/\beta}$	$\frac{\beta(1-u)}{\kappa_\beta} \{-\ln(1-u)\}^{1-1/\beta}$

The Pareto families (Type I or II) with shape parameter $a > 0$ have pdQs defined by $f_a^*(u) = (2 + 1/a)(1-u)^{1+1/a}$. As $a \rightarrow \infty$ the graphs of f_a^* rapidly approach a triangle, the graph of the exponential distribution pdQ. The remaining graphs in Figure 1 are 3:1 mixtures of two normal distributions; Mixture 1 has components $N(0, 1)$ and $N(3, 1)$, and Mixture 2 components are $N(0, 1)$ and $N(3, 1/4^2)$. In summary, all uniform densities transform to the standard uniform; bell-shaped densities with short tails transform roughly to quadratic functions; and exponential distributions correspond to triangular shapes. Mixtures of normal densities appear to transform to a ‘mixture of quadratics’.

1.4 Moments of pdQs

Let $X^* \sim F^*$, $\mu^* = E[X^*]$ and define the k th central moments by $\mu_k^* = E[(X^* - \mu^*)^k] = \int_0^1 (u - \mu^*)^k f^*(u) du$, for $k = 2, 3, \dots$. Denote the standard deviation $\sigma^* = \sqrt{\mu_2^*}$ and the coefficients of skewness and kurtosis by $\gamma_1^* = \mu_3^*/(\sigma^*)^3$ and $\gamma_2^* = \mu_4^*/(\sigma^*)^4$. For all the examples in Table 2, γ_1^* is a good linear predictor of the Hellinger distance of f^* from the class of symmetric distributions on $[0, 1]$, as we will see in Section 4.1.

1.5 Discrete pdQs

Let $\mathcal{X} = \{x_i\}$ be a sequence of distinct real numbers and let $\{p_i\}$ be an associated sequence of non-negative numbers $\{p_i\}$ whose sum is one. Then $\{(x_i, p_i)\}$ defines a *discrete probability distribution*. The class of such distributions is too rich to meaningfully discuss shape via pdQs, so we restrict \mathcal{X} to a *lattice*, a sequence of equally spaced points. By a location-scale change this can be taken to be a subset of the integers. For most distributions of interest to us this domain

Table 2: **Examples of skewness and kurtosis for pdQs of continuous distributions F .**
For the symmetric cases on the left, $\mu^* = 0.5$ and $\gamma_1^* = 0$.

F	σ^*	γ_2^*	F	μ^*	σ^*	γ_1^*	γ_2^*
Beta(2/3,2/3)	0.3561	1.4846	Pareto(0.5)	0.2000	0.1633	1.0498	3.6964
Uniform	0.2887	1.8000	Pareto(1)	0.2500	0.1936	0.8607	3.0952
Laplace	0.2041	2.4000	Pareto(2)	0.2857	0.2130	0.7318	2.7566
Cauchy	0.1808	2.4062	Weibull(2)	0.4557	0.2393	0.1315	2.0714
t_2	0.2041	2.2500	χ_2^2	0.3333	0.2357	0.5657	2.4000
t_3	0.2131	2.1961	χ_3^2	0.3849	0.2354	0.3808	2.2246
t_5	0.2207	2.1527	χ_5^2	0.4205	0.2343	0.2618	2.1513
t_7	0.2240	2.1341	χ_7^2	0.4358	0.2337	0.2116	2.1291
Normal	0.2326	2.0878	Lognormal	0.3415	0.2165	0.5487	2.5035
Logistic	0.2236	2.1429	Extreme Value	0.4444	0.2291	0.1872	2.1459

is of the form $\{0, 1, \dots, n\}$ or $\{0, 1, 2, \dots\}$. Let $\mathcal{D} \subset \mathcal{F}$ be the set of such lattice distributions; they are comprehensively treated by Johnson *et al.* (1993). The pdQ of any $F \in \mathcal{D}$ can now be defined in exactly the same way as for the continuous case, but now the density function is with respect to counting measure, and the density is commonly called the *probability mass function* p and is defined by $p(x_i) = p_i$ for all $x_i \in \mathcal{X}$ and $p(x) = 0$ otherwise.

Definition 2 *The cdf of each $F \in \mathcal{D}$ is a non-decreasing step function with jumps of size p_i at i ; it takes on value $F(x) = S_i = \sum_{j \leq i} p_j$ for x lying in $[i, i + 1)$. The quantile function Q of $F \in \mathcal{D}$ is a monotone increasing left-continuous step function with value i for u lying in $(S_{i-1}, S_i]$. The discrete density quantile function $pQ(u)$ is therefore a step function with value p_i for u lying in $(S_{i-1}, S_i]$. In general, the graph of pQ covers a sequence of adjacent squares with respective sides equal to p_i . Since the sum of the areas of these squares $\kappa = \sum_i p_i^2$ is finite, we define the discrete probability density quantile by $p^*(u) = pQ(u)/\kappa$.*

Given p^* , one can recover p , but not \mathcal{X} . Note that a discrete distribution $p = \{p_i\}$ on a lattice is transformed by this composition and normalization into p^* , which is the density with respect to Lebesgue measure of a continuous distribution with support $[0,1]$. It is a normalized histogram that captures the shape of the original discrete distribution on its support, free of location and scale. We often write f^* for p^* . Examples of discrete pdQs are shown in Figures 2 and 4.

2 Empirical pdQs

Given a sample of data from an unknown $F \in \mathcal{F}$, we want to estimate its pdQ. This will be done separately for the discrete $F \in \mathcal{D}$ and continuous $F \in \mathcal{F}'$ cases.

2.1 An empirical pdQ for discrete distributions

Definition 3 *Given n real numbers which have $M \leq n$ distinct values $x_1 < x_2 < \dots < x_M$, let $f_n(x_m) = n_m/n$ be the relative frequency of occurrences of x_m for $m = 1, \dots, M$. Further let $c_0 = 0$ and $c_m = (\sum_{j=1}^m n_j)/n$ for $m = 1, \dots, M$. Then the empirical pdQ is derived in the same way as the discrete pdQ in Definition 2 to be:*

$$f_n^*(u) = \frac{n \sum_{m=1}^M n_m I\{c_{m-1} < u \leq c_m\}}{\sum_{m=1}^M n_m^2}. \quad (2)$$

If all n observations are distinct, the empirical pdQ in (2) is identically one, just as it is for any other discrete or continuous uniform distribution. For another example, the top left plot of Figure 2 shows the graph of the pdQ of the negative binomial distribution with $r = 2$ and $p = 0.25$. The other plots show empirical pdQs, based on random samples of varying sample sizes. An R script for plotting the empirical pdQ is found in accompanying online material.

2.2 An empirical pdQ for smooth distributions

For smooth distributions $F \in \mathcal{F}'$ we propose estimating $q(u)$ by the estimator already studied by many authors, including Falk (1986), Welsh (1988) and Jones (1992). It is the kernel density estimator that can be written as a linear combination of order statistics:

$$\hat{q}_n(u) = \sum_{i=1}^n X_{(i)} \left\{ k_b \left(u - \frac{(i-1)}{n} \right) - k_b \left(u - \frac{i}{n} \right) \right\}, \quad (3)$$

where b is a bandwidth and $k_b(\cdot) = \frac{1}{b} k(\frac{\cdot}{b})$ is the Epanechnikov (1969) kernel.

It turns out that the asymptotic mean squared error of $\hat{q}(u)$ is minimized when the bandwidth $b(u) = (15/n)^{1/5} \{q(u)/q''(u)\}^{2/5}$. The ratio $q(u)/q''(u)$ is similar in shape to the density quantile $fQ(u) = 1/q(u)$, and hence remarkably stable for F in broad classes such as all symmetric unimodal distributions, or all F with positive unimodal density on $[0, +\infty)$. Prendergast & Staudte (2016) show that by employing the optimal ratio for the Cauchy, one obtains good estimators $\hat{q}(u)$ of $q(u)$ for all F in the first class, while the optimal ratio for the lognormal yields good estimators for all F in the second. In Figure 3 are shown examples of the graphs of $f^*(u) = 1/\{\kappa q(u)\}$ and the estimators $f_n^*(u) = 1/\{\hat{\kappa} \hat{q}_n(u)\}$, $u = 0.005 : 0.995/0.01$, for sample size $n = 1600$. Sample sizes as low as 400 give a good idea of the shape.

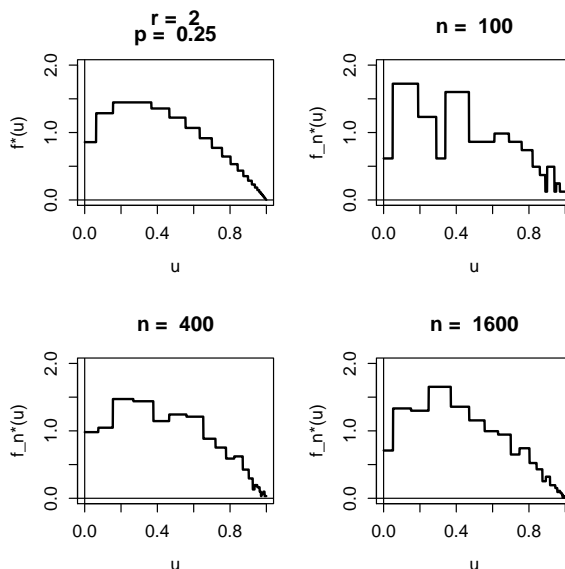


Figure 2: The top left plot shows the graph of the pdQ of the negative binomial distribution with parameters $r = 2$, $p = 0.25$. The remaining empirical pdQ plots defined by (2) in Section 2.1 are based on random samples of size n from this distribution.

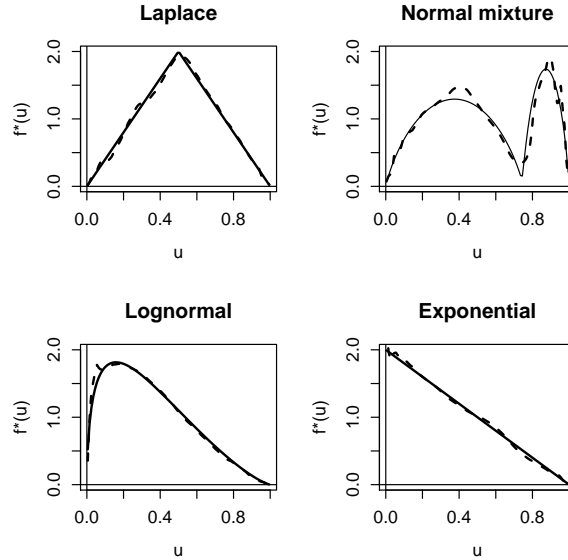


Figure 3: Graphs of $f^*(u)$ (solid lines) and their estimates defined in Section 2.2 (dashed lines). The normal mixture puts weights $3/4, 1/4$ on the standard normal Φ and $\Phi((\cdot - 3)/(1/4))$ respectively. The optimal bandwidth ratio for the Cauchy is used to find the estimates in the top two plots, while the optimal bandwidth ratio for the lognormal is the basis for the others.

3 Applications

We find location- and scale-free global distances between shape families of distributions, which leads to effective fitting of shape families to data.

3.1 Divergence and distance measures

Given densities f_1, f_2 with respect to Lebesgue measure, the *Hellinger distance* between them is defined by $H(f_1, f_2) = [2^{-1} \int \{\sqrt{f_1(x)} - \sqrt{f_2(x)}\}^2 dx]^{1/2}$. The *Kullback-Leibler information* $I(f_1 : f_2)$ in $X \sim f_1$ for discrimination between f_1, f_2 is defined by (Kullback, 1968, p.5) as $I(f_1 : f_2) = \int \ln(f_1(x)/f_2(x)) f_1(x) dx$. The *symmetrized divergence*, or KLD, is defined by $J(f_1, f_2) = I(f_1 : f_2) + I(f_2 : f_1)$. We often abbreviate $H(f_1, f_2)$ to $H(1, 2)$, $I(f_1 : f_2)$ to $I(1 : 2)$ and $J(f_1, f_2)$ to $J(1, 2)$. Further, we denote by $H^*(1, 2)$ the Hellinger metric applied to the pdQs f_1^*, f_2^* of f_1, f_2 , and similarly for $I^*(1 : 2)$ and $J^*(1, 2)$. An advantage of working with f^* s over f s is that the pdQs for both discrete and continuous F are densities with respect to Lebesgue measure, so the Hellinger distance or KLD between their pdQs can be informative.

3.2 Probabilistic examples

Ex. 1: Rate of convergence in Hellinger distance of Poisson from normality.

It is well known (Johnson *et al.*, 1993, p.161) that $X \sim \text{Poisson}(\lambda)$ approaches the normal distribution as $\lambda \rightarrow \infty$ in that $(X - \lambda)/\sqrt{\lambda} \rightarrow Z \sim \Phi$ in distribution. And numerical computations show that the Hellinger distance between the Normal pdQ and that of the $\text{Poisson}(\lambda)$ distribution is $H = H(f_\lambda^*, \varphi^*) \approx 0.17077/\sqrt{2.4\lambda - 1}$ for $1 \leq \lambda \leq 100,000$.

Table 3: For selected values of ν are shown the λ_{\min} to 3 decimal places that minimizes the Hellinger distance of the pdQs for the symmetric Tukey(λ) distributions from the pdQ of Student's t-distribution with ν degrees of freedom. Also shown are the minimum Hellinger distances.

ν	0.5	1	2	3	4	5	6	7	12	24	100
λ_{\min}	-1.881	-0.867	-0.357	-0.188	-0.104	-0.053	-0.020	0.004	0.063	0.104	0.135
H_{\min}	0.005	0.005	0.004	0.003	0.003	0.003	0.002	0.002	0.002	0.001	0.001

Ex. 2: Discretized exponential.

Given $X \sim \text{Exponential}(1)$, for $0 < r \leq 1$ let $Y_r = \lfloor rX \rfloor \sim \text{Geometric}(p_r)$, with $p_r = 1 - e^{-r}$. Then the Hellinger distance of X^* from Y_r^* is $H_r \approx r/10$; and the root-KLD divergence $\sqrt{J_r} \approx 3r/11$, for $0 < r \leq 1$. This example illustrates that one can quantify the Hellinger distance between a continuous distribution and a discrete approximation to it.

Ex. 3: Matching symmetric Tukey distributions with Student's t-distributions.

Student's t-distributions are well approximated by certain symmetric Tukey(λ) distributions, see ?, Joiner & Rosenblatt (1971), ? and references therein. These authors used expected ranges or specific tail probabilities to match distributions; and in particular find that for the Cauchy ($\nu = 1$) the symmetric Tukey distribution with $\lambda = -1$ is close to it, while for the Normal ($\nu \rightarrow \infty$) the Tukey with $\lambda = 0.14$ is quite close. Here we find the best global fits using metrics on the respective pdQs, and obtain very similar results. In Table 3 are listed the $\lambda = \lambda_{\min}(\nu)$ that minimize the Hellinger distance between the pdQs of the Tukey(λ) family and the pdQ of the Student's t distribution with ν df. The minimum distance H_{\min} is also shown. For the normal distribution we found $\lambda_{\min}(\infty) = 0.14435$ with $H_{\min} = 0.0010$. A good approximation for $\nu \geq 12$ is given by $\lambda_{\min} = 0.14435 - 1/(1.07\nu)$. Minimizing the KLD instead of the Hellinger metric led to the same results for λ_{\min} .

3.3 Data examples

Robust global fitting of shape parameter families to data is possible by minimizing the Hellinger distance of the model pdQ to the empirical pdQ, as we now demonstrate for three important shape families.

Ex. 4: Fitting symmetric Tukey models to data.

A standard method of fitting a family of distributions indexed by a shape parameter to data is due to Filliben (1975). He suggested finding the correlation coefficient between the ordered data and the quantiles determined by the family for a range of values of the shape parameter and then constructing the 'probability plot correlation coefficient' (ppcc): the correlation coefficient as a function of shape parameter. The shape parameter that maximizes the coefficient is his proposed ppcc estimate. This method is often applied to symmetric-looking data to fit a member of the Tukey(λ) family, and if an estimate of λ were near -1 , (or 0.14), say, it is suggested to assume a Cauchy (or normal) model, see the discussion in Example 3 and Table 3. Location and scale estimates are then obtained by regressing the sorted data on the quantiles of the chosen shape model.

As an alternative method of fitting a family of distributions indexed by a shape parameter to data, we propose finding the empirical pdQ $f_n^*(u) = 1/\{\hat{\kappa}\hat{q}_n(u)\}$ of Section 2.2 for u in a grid on $[0,1]$. This nonparametric density estimate requires a sample size of at least 500. Then,

for each shape parameter λ , say, in a large range of values, compute the Hellinger distance $H_\lambda = H(f_n^*, f_\lambda^*)$ of f_n^* from the model pdQ f_λ^* . The λ that minimizes this distance will be called the H -pdQ *goodness-of-fit estimate* of λ .

Both methods require a search over a grid of λ values and we recommend that this be done in two stages: first, for a rough grid over a large range, say increments of size 0.2 over $[-10, 10]$; and second, over a narrow range around the first estimate with increments of size 0.01, say. In our simulation study we made one pass with increments 0.01 over $[-10, 10]$. For sample size 500 the run time for this search was approximately 0.6 second. To compare these methods we ran 400 replications of an experiment with sample sizes 500 selected at random from the symmetric Tukey(λ) distribution using the R package `gld` due to ? with the ? parameterization. The R command to obtain a sample of simulated data x is `x <- rg1(500, c(0,lambda,lambda,lambda), param = "rs", lambda5 = NULL)`. The choices of λ listed in Table 4 are representative of very long, long, normal and truncated tails, respectively, also discussed later in Section 5.

The results of fitting these data sets by the methods `ppcc` and H -pdQ are summarized in Table 4. In particular, we list the empirical standard errors (SE equals the square root of the sample variance plus squared estimated bias). The rows corresponding to $\lambda = -1$ and $\lambda = -2$ suggests that for long and very long tails, the pdQ approach is much more efficient at identifying the data source. However, for the cases where the data are approximately normal or have truncated tails, there is little to choose between the methods.

Table 4: For selected values of λ are shown summary results for 25 competing estimates (`ppcc` and H -pdQ) based on samples of size 500 from the Tukey(λ).

λ	Method	SE	mean	sd	min	max
-2	<code>ppcc</code>	2.61	-3.31	2.26	-10.00	-0.86
	H -pdQ	0.18	-2.02	0.18	-2.76	-1.52
-1	<code>ppcc</code>	1.46	-1.72	1.27	-8.41	-0.63
	H -pdQ	0.11	-1.02	0.11	-1.34	-0.68
0.14	<code>ppcc</code>	0.05	0.12	0.05	0.01	0.28
	H -pdQ	0.06	0.14	0.06	0.05	0.29
3	<code>ppcc</code>	0.94	2.67	0.88	0.45	3.52
	H -pdQ	0.60	2.77	0.55	0.52	3.43

Ex. 5: Fitting Weibull models to data.

Another shape family that is often fitted to lifetime or income data is the Weibull model with shape parameter β . We compare three methods: the `ppcc` and H -pdQ methods just described in the last example; the third is the maximum likelihood (MLE) approach, available through the command `fitdistr(x,"weibull")` on the software (R, 2013, Core Development Team) with the internal package MASS, ?; it assumes $x > 0$ and returns both scale and shape MLEs and their standard errors based on the observed information matrix.

The summary results for 400 replications of sample size 500 from six data configurations are listed in Table 5. For the Weibull $\beta = 1$ (exponential) model the MLE approach performs best, having the smallest SE, while the H -pdQ method is the second best performer. In the second and third configurations of 5% contaminated data, the MLE and H -pdQ methods are comparable, while the `ppcc` method is badly affected by a few outliers. The simulations for $\beta = 2$ show that the MLE approach can also perform poorly for contaminated data.

Similar results to those above were obtained by fitting the Gamma shape family.

Table 5: Summary results of competing estimates (ppcc, H -pdQ and MLE) of the Weibull shape parameter β based on 400 replications of samples of size 500 from the Weibull W_β with $\beta = 1, 2$ distributions; and also from 95:05 mixture distributions of W_β with contamination from the standard lognormal (LN) and then such contamination multiplied by two (2LN),

Data Source	Method	SE	mean	sd	min	max
W_1	ppcc	0.09	0.96	0.09	0.66	1.25
	H -pdQ	0.06	0.97	0.06	0.64	1.09
	MLE	0.04	1.00	0.04	0.89	1.12
$0.95 W_1 + 0.05(LN)$	ppcc	0.17	0.89	0.14	0.22	1.17
	H -pdQ	0.05	0.98	0.05	0.81	1.14
	MLE	0.04	1.00	0.04	0.88	1.10
$0.95 W_1 + 0.05(2LN)$	ppcc	0.42	0.64	0.21	0.10	1.09
	H -pdQ	0.06	0.97	0.05	0.79	1.10
	MLE	0.07	0.94	0.05	0.79	1.04
W_2	ppcc	0.15	1.99	0.15	1.56	2.47
	H -pdQ	0.18	2.12	0.14	1.71	2.52
	MLE	0.07	1.96	0.07	1.78	2.23
$0.95 W_2 + 0.05(LN)$	ppcc	1.12	0.99	0.48	0.10	2.13
	H -pdQ	0.12	1.97	0.12	1.66	2.40
	MLE	0.39	1.65	0.19	1.01	2.10
$0.95 W_2 + 0.05(2LN)$	ppcc	1.61	0.40	0.22	0.10	1.29
	H -pdQ	0.15	1.89	0.11	1.50	2.16
	MLE	0.68	1.34	0.16	0.95	1.80

Ex. 6: Fitting shape models to wool fibre diameter data.

Raw wool is routinely classified by the distribution of fibre diameters, measured in microns. A typical example of 4817 measurements obtained by laser scanning technology is given in Appendix 7.1. Of main interest to wool assessors is the mean diameter $\bar{x} = 25.08$, the standard deviation $s = 5.388$ and the coefficient of variation $cv = 0.215$, as well as percentages of relatively large fibres that can cause prickliness in finished woolen goods. Here we fit parametric models to these data using the three methods described above.

Table 6: The best fitting Weibull(β) and Gamma(α) models to the wool fibre diameter data are listed, along with location and scale estimates obtained by regressing the quantiles of the sorted data on the quantiles of the respective fitted shape models. The values of H are Hellinger distances of the empirical pdQ of Section 2 from each of the pdQs with estimated shape parameters.

Family	Method	Shape	Location	Scale	H
Weibull	ppcc	2.44	12.80	13.85	0.0360
	H -pdQ	2.76	11.38	15.40	0.0323
	MLE	4.82	2.66	24.47	0.0595
Gamma	ppcc	22.21	-0.26	1.14	0.0234
	H -pdQ	35.75	-7.09	0.89	0.0220
	MLE	21.67	0.03	1.15	0.0236

For the Weibull family, the ppcc and H -pdQ results are very similar. The MLE estimate of β is quite different, because it was obtained by the MLE optimization method that assumes zero location and estimates scale and shape simultaneously. That is why the regression results for location and scale shown in Table 6, namely 2.66 and 24.47 are close to zero and the MLE estimate of scale 27.26, respectively. The Hellinger distance of the MLE fitted pdQ from the

empirical pdQ is almost twice that of the distances for the other two fitted models.

For the Gamma models, the Hellinger distances for all three methods are all about 1/2 those for the Weibull models. QQ-plots for these six best fitting distributions reveal that the Weibull models all fit quite badly; while for the fitted gamma models all QQ-plots are almost linear. Examples of some QQ-plots are in Figure 6 of Appendix 7.1. For the gamma family, a wide range of shape parameters leads to a good fit; and an examination of the ppcc plot reveals it is almost flat for $20 < \alpha < 50$. Also, the corresponding Hellinger distances are almost the same for this range of α .

4 Measuring asymmetry in a pdQ

In addition to skewness and kurtosis of pdQs, the ‘shape’ can be described by the degree of asymmetry, the location of modes, and the tail behavior of f^* at 0 and 1.

4.1 Finding the closest symmetric distribution to a pdQ

One can measure the skewness of a pdQ with the coefficient γ_1^* as in Table 1, or with many other definitions found in Staudte (2014). However, asymmetry entails more than skewness, because asymmetric distributions can have 0 skewness. Here we measure the asymmetry of a pdQ by finding its distance or divergence to the class of symmetric distributions on $[0,1]$. It is shown in Theorem 3.2 of Withers & Nadarajah (2010) that if f_1, f_2 are densities with respect to Lebesgue measure and f_2 is assumed to be symmetric about 0, then the closest such f_2 to f_1 in terms of minimizing the Hellinger distance is given by $f_2(x) = \alpha^2(x)/d$ where $\alpha(x) = \{\sqrt{f_1(x)} + \sqrt{f_1(-x)}\}/2$ and $d = 2 \int_0^{+\infty} \alpha^2(x) dx$. Consequently, if f^* is an arbitrary pdQ, the Hellinger-closest symmetric distribution is given by $f_{\text{symm}}^*(u) = \{\alpha^*(u)\}^2/d^*$ where $\alpha^*(u) = \{\sqrt{f^*(u)} + \sqrt{f^*(1-u)}\}/2$ and $d^* = \int_0^1 \{\alpha^*(u)\}^2 du$. The actual Hellinger distance $H_{\min}(f^*) = H(f^*, f_{\text{symm}}^*)$ of f^* from the class of symmetric distributions is determined by:

$$2\{1 - H_{\min}^2(f^*)\}^2 = 1 + \int_0^1 \sqrt{f^*(u)f^*(1-u)} du . \quad (4)$$

Some examples are shown in Figure 4.

Withers & Nadarajah (2010) also find the closest symmetric distribution to a given one in the sense of minimizing the Kullback-Leibler divergence $I(2 : 1)$. Their result is extended to minimizing $J(1, 2)$ in the following proposition.

Proposition 1 *Given f_1, f_2 probability densities with respect to Lebesgue measure, and assume that f_2 is symmetric about 0. Then*

- (a) *The f_2 that minimizes $I(2 : 1)$ is given by $f_2(x) = \nu(x)/d$, where $\nu(x) = \sqrt{f_1(x)f_1(-x)}$ and $d = 2 \int_0^{+\infty} \nu(x) dx$.*
- (b) *The f_2 that minimizes $I(1 : 2)$ is given by $f_2(x) \equiv \bar{f}_1(x) \equiv \{f_1(x) + f_1(-x)\}/2$.*
- (c) *The f_2 that minimizes $J(1, 2)$ is given by $f_2(x) = \beta(x)/d$ where $\beta(x)$ is the solution to:*

$$\beta(x) = \nu(x) \exp \{ \bar{f}_1(x)/\beta(x) \} ; \quad (5)$$

and $d = 2 \int_0^\infty \beta(x) dx$.

The proof of Proposition 1 is in the Appendix 7.2, along with an algorithm for computing the minimizer of J guaranteed by Part (c) and two illustrative examples.

In our applications of Proposition 1 to pdQs f_1^*, f_2^* on the unit interval, where symmetry takes place about $1/2$, $\bar{f}_1(x) \equiv \{f_1(x) + f_1(-x)\}/2$ becomes $\bar{f}_1^*(u) \equiv \{f_1^*(u) + f_1^*(1-u)\}/2$, and similarly $\nu(x)$ becomes $\nu^*(u) \equiv \sqrt{f_1^*(u)f_1^*(1-u)}$. The minimum divergences realized in applying parts (a)-(c) of Proposition 1 to the pdQs are denoted, respectively, $I_{:1}^*$, $I_{1:}^*$ and J^* .

Table 7: The coefficient of skewness γ_1^* of f^* taken from Table 2 is listed, along with the $H^* = H_{\min}(f^*)$ of (4), and the minimum divergences $I_{1:}^*$, $I_{:1}^*$ and J^* of Proposition 1 applied to $f_1^* = f^*$.

F	γ_1^*	H^*	$I_{1:}^*$	$I_{:1}^*$	J^*
Pareto(0.5)	1.0498	0.4421	0.5401	1.2224	2.1589
Pareto(1)	0.8607	0.3660	0.4077	0.6931	1.2710
Pareto(2)	0.7318	0.3094	0.3107	0.4535	0.8507
Weibull(2)	0.1315	0.0672	0.0178	0.0182	0.0363
χ_2^2	0.5657	0.2349	0.1931	0.2416	0.4646
χ_3^2	0.3808	0.1687	0.1061	0.1191	0.2326
χ_5^2	0.2618	0.1191	0.0548	0.0580	0.1145
χ_7^2	0.2116	0.0970	0.0368	0.0382	0.0757
Lognormal	0.5487	0.2386	0.2014	0.2500	0.4747
Extreme Value	0.1872	0.0855	0.0287	0.0295	0.0587

In Table 7 are listed the values of some possible measures of asymmetry for a given pdQ f^* for f belonging to an asymmetric location-scale family F . These values are positively correlated, and γ_1^* , H^* , $\sqrt{I_{1:}^*}$, $\sqrt{I_{:1}^*}$ and $\sqrt{J^*}$ are very highly correlated, as shown in Figure 5.

To show that $H^* = 0.43 \cdot |\gamma_2^*|$ is only an approximation on the class of pdQs, consider the power function family $F_b(u) = u^b$, $0 < u < 1$, $b > 0$, which is also the Beta($b, 1$) family. Assuming $b > 1/2$, it has pdQ $f_b^* = f_{b^*}$ with $b^* = 2 - 1/b$, so $f_b^* \sim \text{Power}(b^*)$, or Beta($b^*, 1$). The skewness coefficient of the Beta family is known (Johnson *et al.*, 1995, p.217), and in this

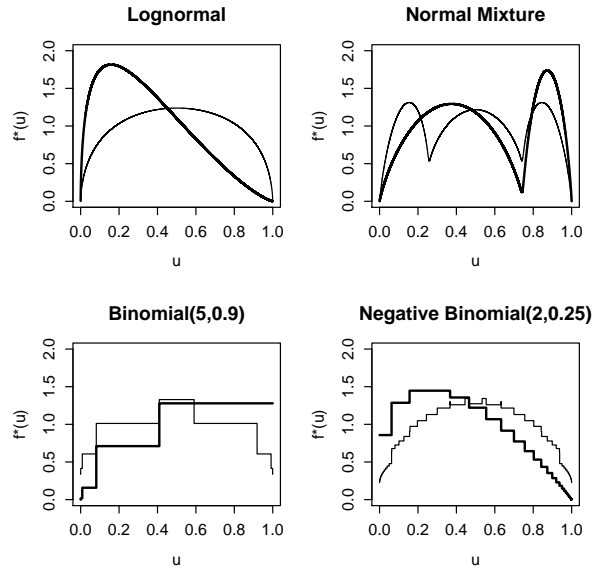


Figure 4: Graphs of $f^*(u)$ in thick black lines and their respective closest (in the Hellinger distance) symmetric distributions f_{symm}^* in thin lines. The normal mixture puts weights $3/4, 1/4$ on the standard normal Φ and $\Phi((\cdot - 3)/(1/4))$ respectively. The respective Hellinger distances to the symmetric class on $[0, 1]$ in the four cases are 0.2386 , 0.1255 , 0.1376 and 0.1443 .

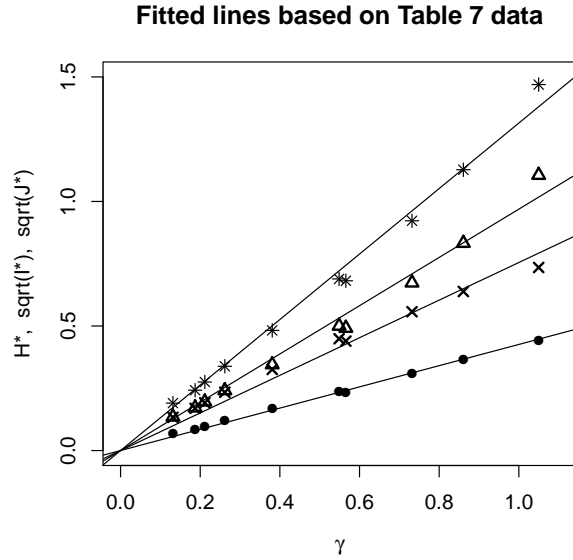


Figure 5: Plots of H^* versus $\gamma \equiv \gamma_1^*$ in circles, and $\sqrt{I_{1:}^*}$, $\sqrt{I_{:1}^*}$ and $\sqrt{J^*}$ against γ in crosses, triangles and asterisks, respectively, based on results in Table 7. Superimposed are their least-squares lines through the origin, with approximate coefficients 0.43, 0.75, 0.97 and 1.31.

case $\gamma_1(b^*) = 2(1 - b^*)\sqrt{1 + 2/b^*}/(b^* + 3)$, for $\beta^* \in (0, 2]$. It is monotone decreasing in b^* over this range with limiting values $\gamma_1(0+) = +\infty$ and $\gamma_1(2) = -2\sqrt{2}/5$.

To find the Hellinger distance $H_{\min}(f_{b^*})$ from the symmetric class, we need

$$\int_0^1 \sqrt{f_b^*(u)f_b^*(1-u)} du = b^* \text{Beta} \left(\frac{b^* + 1}{2}, \frac{b^* + 1}{2} \right) = \frac{\Gamma^2 \left(\frac{b^* + 1}{2} \right)}{\Gamma(b^*)}.$$

This quantity approaches $\pi/4$ as $b^* \rightarrow 2$, and using (4) the minimum Hellinger distance to a symmetric distribution approaches $\sqrt{1 - \sqrt{(1 + \pi/4)/2}} = 0.2348882$. The ratio $|\gamma_1(b^*)|/H_{\min}(f_{b^*}) \rightarrow 0.415228$ as $b^* \rightarrow 2$, a value not far from the gradient 0.43 fitted to the 10 models in Figure 5. The ratio $|\gamma_1(b^*)|/H_{\min}(f_{b^*})$ is indeed greater than 0.37 for $b^* > 1$, but for $b^* \leq 2/3$ this ratio falls below $1/3$. This example suggests that the approximation $H_{\min}(f^*) \approx 0.43|\gamma_1(f^*)|$ may only hold for bounded f^* .

5 Classification by tail-weight

We focus on the right-hand tails, leaving the adjustments for left-hand tails to the reader. Recall that $f^*(u) = fQ(u)/\kappa$ so $f^*(u)$ is the rate at which the density f is accumulating probability at its u th quantile. Given f^*, g^* with $f^*(u)/g^*(u) > 1$ for u approaching 1, we would say f has the *shorter* right tail, because it reaches its large quantiles faster than g reaches its corresponding large quantiles. This enables one to partially order tails of all densities f with support bounded on the right, which is perhaps the least interesting case. We somewhat arbitrarily define such f to have ‘short’ right tails.

The more interesting cases are for f with unbounded support to the right, in which case $f^*(1) = 0$. The first derivative $(f^*)'(u) = f'(Q(u))q(u) = -J(u)/\kappa$, where $J(u) = -(f'/f)(Q(u))$ is the score function for location-scale families that plays an important role in classical non-parametric statistics, see e.g. Hajek & Sidak (1967). Now, because $f^*(1) = 0$,

$$(f^*)'(1) = \lim_{u \rightarrow 1} \frac{f^*(1) - f^*(u)}{1 - u} = \lim_{u \rightarrow 1} \frac{-fQ(u)}{\kappa(1 - u)} \leq 0. \quad (6)$$

Parzen (1979) observes that when $fQ(u)/(1 - u)^\alpha$ approaches a finite positive limit for some positive α , then the intervals $0 < \alpha < 1$, $\alpha = 1$ and $\alpha > 1$ correspond to the statistician’s

perception that probability laws have three types of behavior: short, medium (exponential) and long, respectively. Note that $(f^*)'(1)$ in (6) is essentially case $\alpha = 1$.

5.1 Definitions and properties

The above considerations plus examination of several examples below lead us to introduce a more detailed description of tail behavior, based on derivatives of the pdQ at the boundaries. This system not only divides tails into classes based on their relative rate of convergence to 0 relative to the exponential, but also seeks within classes to provide an absolute measure of tail-weight within classes.

Definition 4 For $n \geq 1$ define $(f^*)^{(n)}(1) \equiv \lim_{u \uparrow 1} (f^*)^{(n)}(u)$, assuming these derivatives exist as finite numbers for u near one and their limits as $u \rightarrow 1$ exist as finite or infinite values.

Let n^* be the smallest integer $n \geq 1$ for which $(f^*)^{(n)}(1) \neq 0$. If n^* exists, the right tail is of n^* -order; otherwise it is of infinite $*$ -order. The tail is called medium, long or very long respectively, if $n^* = 1, 2$ or $n^* \geq 3$.

A sampling of examples is in Table 8. Note that for medium tails (the case $n^* = 1$), one has $(f^*)(1) = 0$ and $(f^*)'(1) \neq 0$, but this derivative at 1 must be non-positive. The larger the magnitude $|(f^*)'(1)|$, the shorter the tail. Similarly for long-tailed pdQs, the case $n^* = 2$, one has $(f^*)(1) = (f^*)'(1) = 0$ and $(f^*)''(1) \neq 0$. Now $(f^*)'(u) \leq 0$ for u near 1, so its derivative $(f^*)''(1)$ will be non-negative or $+\infty$.

The pdQs are not always ordered because different pdQs, such as the normal and Tukey with $0 < \lambda < 1$, both have infinity limits of their derivatives as $u \rightarrow 1$. One could order such pdQs by comparing the ratio of their derivatives $(f^*)'(u)/(g^*)'(u)$ as $u \rightarrow 1$, and similarly for distributions with long or very long tails, but we will not pursue this here.

5.2 Examples

The lognormal distribution.

The lognormal pdQ is from Table 1 given by $f^*(u) = c\varphi(z_u)\exp(-z_u)$, where $z_u = \Phi^{-1}(u)$ and $c = 1/\kappa = 2\sqrt{\pi}\exp(-0.25)$. Thus $(f^*)'(u) = -c\exp(-z_u)(1+z_u)$, which approaches 0 as $u \rightarrow 1$. Further, $(f^*)''(u) = cz_u\exp(-z_u)/\varphi(z_u)$, which approaches $+\infty$ as $u \rightarrow 1$ so the lognormal right tail is 'long'.

Student's t-distribution with $\nu = 2$ degrees of freedom.

? gives the density quantile function of Student's t-distribution with $\nu = 2$ degrees of freedom, and by numerical integration one can find the normalizing constant $\kappa = 0.20826$ to obtain its pdQ $f^*(u) = fQ(u)/\kappa = \{2u(1-u)\}^{3/2}/\kappa$. The reader can readily verify that $f^*(1) = 0$, $(f^*)'(1) = 0$ and $(f^*)''(1) = +\infty$ so this f^* has long tails, but shorter than those of the Cauchy distribution. The tail behavior for large ν may possibly be found using results in Schlüter & Fischer (2012).

The Pareto distributions.

The Pareto(a) family, with $a > 0$ has $f_a^*(u) = (2 + \frac{1}{a})(1-u)^{1+1/a} \rightarrow 0$ as $u \rightarrow 1$. So $(f_a^*)'(u) = -(1 + \frac{1}{a})(2 + \frac{1}{a})(1-u)^{1/a} \rightarrow 0$ as $u \rightarrow 1$, again, for all $a > 0$. Therefore $n^* \geq 2$ and the

Table 8: **Right-tail behavior of some continuous distributions.** The pdQ s are listed in Table 1. Note that if $f^*(1) = 0$, then $(f^*)'(1) \leq 0$.

tail	F	$(f^*)'(1)$	$(f^*)''(1)$
	Normal	$-\infty$	-
	Tukey(λ), $0 < \lambda < 1$	$-\infty$	-
	Logistic (Tukey(0))	-6	-
Medium	Extreme Value	-4	-
	Laplace	-2	-
	Exponential	-2	-
	Pareto(a), $1 < a$	0	$+\infty$
	Lognormal	0	$+\infty$
Long	Tukey(λ), $-1 < \lambda < 0$	0	$+\infty$
	Cauchy	0	$4\pi^2 = 39.48$
	Tukey(-1)	0	33.69
	Pareto(1)	0	6
	Tukey(λ), $\lambda < -1$	0	0
Very long	Pareto(a), $0 < a < 1$	0	0

right-hand tails are ‘long’ or ‘very long’. The second derivative satisfies, as $u \rightarrow 1$

$$(f_a^*)''(u) = \frac{(1+a)(1+2a)}{a^3} (1-u)^{1/a-1}$$

$$\rightarrow \begin{cases} 0, & 0 < a < 1 \\ 6, & a = 1 \\ +\infty, & 1 < a. \end{cases}$$

Therefore the tails are long ($n^* = 2$) if and only if $a \geq 1$ and otherwise they are very long ($n^* \geq 3$). Further, $(f_a^*)^{(n)}(1) = 0$ for $0 < a < 1/2^{n-1}$ for all $n \geq 2$. Thus there exist distributions with tails of every n^* -order.

The symmetric Tukey(λ) distributions.

The Tukey(λ) family provides a wide range of tail-weights. Starting with f_λ^* from Table 1, the first two derivatives are:

$$\begin{aligned} \kappa_\lambda f_\lambda^*(u) &= \{u^{\lambda-1} + (1-u)^{\lambda-1}\}^{-1} \\ \kappa_\lambda (f_\lambda^*)'(u) &= (1-\lambda)(\kappa_\lambda f_\lambda^*(u))^2 \{u^{\lambda-2} - (1-u)^{\lambda-2}\} \\ \kappa_\lambda (f_\lambda^*)''(u) &= 2(1-\lambda)^2 \frac{\{u^{\lambda-2} - (1-u)^{\lambda-2}\}^2}{\{u^{\lambda-1} + (1-u)^{\lambda-1}\}^3} + (1-\lambda)(\lambda-2) \frac{\{u^{\lambda-3} + (1-u)^{\lambda-3}\}}{\{u^{\lambda-1} + (1-u)^{\lambda-1}\}^2} \\ &\sim 2(1-\lambda)^2 \frac{\{1 - (1-u)^{\lambda-2}\}^2}{\{1 + (1-u)^{\lambda-1}\}^3} + (1-\lambda)(\lambda-2) \frac{\{1 + (1-u)^{\lambda-3}\}}{\{1 + (1-u)^{\lambda-1}\}^2}, \end{aligned}$$

as $u \rightarrow 1$. From the first equation above $f_\lambda^*(1) > 0$ if and only if $\lambda \geq 1$ and in this case ‘short’ tails are obtained. For $\lambda < 1$ examination of the first derivative $(f_\lambda^*)'(u)$ as $u \uparrow 1$ yields the value 0 for $\lambda < 0$, the value -6 for $\lambda = 0$ and $-\infty$ for $0 < \lambda < 1$; in these last two cases $n^* = 1$ and the tails are ‘medium’. For $\lambda < 0$ one can see from the last displayed expression that $(f_\lambda^*)''(1) = 0$ when $\lambda < -1$ and so the tails are ‘very long’. For $-1 \leq \lambda < 0$ the second derivative $(f_\lambda^*)''(1) > 0$ and the tails are ‘long’. In particular, for $\lambda = -1$ one has $(f^*)''(1) \approx 33.7$ which is not far from that of the Cauchy $4\pi^2$, see Table 8.

6 Summary and further research

The pdQ transformation from f to f^* is quite powerful, and allows for a different look at distributional shapes, on a common finite domain $[0,1]$ where location, scale and gaps are not distractions. This has enabled us to compare discrete with continuous distributions by applying the Hellinger metric and/or Kullback-Leibler divergences to their respective pdQs. It also facilitated finding ‘closest’ symmetric distributions to a given pdQ, so that they could be ordered by their distance or divergences from the symmetric class. Further, we have classified tail behavior using boundary derivatives of the pdQs.

With regard to inference, we defined empirical pdQs in both the discrete and continuous case. The latter are based on quantile density estimators of Prendergast & Staudte (2016), and generally require moderately large sample sizes of 500 or more. Given such a sample, we showed that one could fit a parametric shape model to it by minimizing over the shape parameter the Hellinger distance of the proposed model pdQ from the empirical pdQ. This H -pdQ method is location-scale free, and we demonstrated its effectiveness relative to the ppcc method of Filliben (1975) for the symmetric Tukey(λ) family as well as gamma and Weibull models. The new method is a *global* density fitting technique, but rather than finding the distance of an empirical density $f_n(x)$ with a proposed $f(x)$ on an infinite domain, which is hard to do, it finds the distance between the normalized $f_n(Q_n(u))$ and a proposed $f(Q(u))$ on $[0,1]$, in effect comparing the densities f_n and f at their respective quantiles. This procedure appears more resistant to outliers than traditional fitting methods such as maximum likelihood.

In the asymmetric case one could similarly try fitting the generalized lambda distributions without having to estimate location and scale; background material is in Gilchrist (2000), Karian & Dudewicz (2000), ? and Prendergast & Staudte (2016). Another family with two shape parameters Dagum (1977) might also be fitted by the H -pdQ technique.

As a specific application, given wool fibre diameter data and hence an empirical pdQ, we showed that one could globally fit shape families such as Gamma and Weibull to it. When parametric models do not fit such fibre diameter data well, a non-parametric approach to classifying wool is possible using quantile methods. For example one could replace the mean by the median and the coefficient of variation by an interquantile range divided by the median, which is just the reciprocal of the standardized median investigated by Staudte (2013).

With regard to theoretical research on pdQs, what happens with another application of the pdQ-transformation to $f^{**} = (f^*)^*$? And further, with n iterations $f^{(n+1)*} = (f^{n*})^*$ for $n \geq 2$, and $n \rightarrow \infty$? Preliminary work suggests that under weak conditions, such as the n th power integrability of f for all n , the limit $\lim_{n \rightarrow \infty} f^{(n)*}(u)$ exists and is the ‘shapeless’ uniform distribution on $[0,1]$.

While the pdQs of discrete distributions are of interest, we have not delved into them much here. For example, the moments in Table 2 could include those of discrete distributions. It would also be of interest to extend the tail-weight analysis of Section 5 to discrete distributions, although the boundary derivatives could not be found as limits of derivatives near the boundary.

With regard to right tail-weight, those pdQs of n^* -order, but infinite n^* derivative at 1, could be compared by looking at the relative rates at which these n^* derivatives approach infinity. It would be of interest to include Student’s t_ν pdQs for $\nu > 1$ degrees of freedom, as well as many other long and very long tailed distributions, in Table 8.

Extending the concept of pdQs to the multivariate case appears feasible, if challenging, and likely to lead to numerous applications for multivariate data, because the metrics, divergences and empirical pdQs are still available.

: Acknowledgments: The author is indebted to the Editors and the referees whose detailed comments and suggestions greatly improved the clarity of this manuscript.

References

- BOTHA, A.F., & HUNTER, L. 2010. The measurement of wool fibre properties and their effect on worsted processing performance and product quality. part 1: The objective measurement of wool fibre properties. *Textile Progress*, **42**(4), 227–339.
- DAGUM, C. 1977. A new model of personal income distribution: Specification and estimation. *Economie Appliquée*, **30**, 413–437.
- EPANECHNIKOV, V.A. 1969. Nonparametric estimation of a multivariate probability density. *Theory of Probability and its Applications*, **14**, 153–158.
- FALK, M. 1986. On the estimation of the quantile density function. *Statistics and Probability Letters*, **4**, 69–73.
- FILLIBEN, J.J. 1975. The probability plot correlation coefficient test for normality. *Technometrics*, **17**, 111–117.
- FREIMER, M., MUDHOLKAR, G.S., KOLLIA, G., & LIN, C.T. 1988. A study of the generalized Tukey lambda family. *Communications in Statistics - Theory and Methods*, **17**, 3547–3567.
- GILCHRIST, W. 2000. *Statistical Modelling with Quantile Functions*. London: Chapman and Hall/CRC.
- HAJEK, J., & SIDAK, Z. 1967. *Theory of Rank Tests*. New York: Academic Press.
- JOHNSON, N.L., KOTZ, S., & KEMP, A.W. 1993. *Univariate Discrete Distributions*. second edn. New York: John Wiley & Sons.
- JOHNSON, N.L., KOTZ, S., & BALAKRISHNAN, N. 1994. *Continuous Univariate Distributions*. Vol. 1. New York: John Wiley & Sons.
- JOHNSON, N.L., KOTZ, S., & BALAKRISHNAN, N. 1995. *Continuous Univariate Distributions*. Vol. 2. New York: John Wiley & Sons.
- JOINER, B.L., & ROSENBLATT, J.R. 1971. Some properties of the range in samples from Tukey’s symmetric lambda distributions. *Journal of the American Statistical Association*, **66**, 394–399.
- JONES, M.C. 1992. Estimating densities, quantiles, quantile densities and density quantiles. *Annals of Institute of Statistical Mathematics*, **44**(4), 721–727.
- KARIAN, Z.A., & DUDEWICZ, E.J. 2000. *Fitting Statistical Distributions: The Generalized Lambda Distribution and Generalized Bootstrap Methods*. Boca Raton: Chapman and Hall.
- KING, R., DEAN, B., & KLINKE, S. 2014. *gld: Estimation and use of the generalised (Tukey) lambda distribution*. R package version 2.2.1.
- KULLBACK, S. 1968. *Information Theory and Statistics*. Mineola: Dover.
- PARZEN, E. 1979. Nonparametric statistical data modeling. *Journal of the American Statistical Association*, **7**, 105–131.
- PARZEN, E. 2004. Quantile probability and statistical data modeling. *Statistical Science*, **4**, 652–662.

- PRENDERGAST, L.A., & STAUDTE, R.G. 2016. Exploiting the quantile optimality ratio in finding confidence intervals for a quantile. *Stat*, **5**(1), 70–81.
- R, CORE TEAM. 2013. *R: A language and environment for statistical computing*. R Foundation for Statistical Computing, Vienna, Austria.
- SCHLÜTER, S., & FISCHER, M. 2012. A tail quantile approximation for the student t distribution. *Communications in Statistics: Theory and Methods*, **41**(15), 2617–2625.
- STAUDTE, R.G. 2013. Distribution-free confidence intervals for the standardized median. *Stat*, **2**(1), 184–196.
- STAUDTE, R.G. 2014. Inference for quantile measures of skewness. *Test*, **23**(4), 751–768.
- TUKEY, J.W. 1962. The future of data analysis. *Annals of Mathematical Statistics*, **33**, 1–67.
- TUKEY, J.W. 1965. Which part of the sample contains the information? *Proceedings of the Mathematical Academy of Science USA*, **53**, 127–134.
- TUKEY, J.W. 1977. *Exploratory Data Analysis*. Reading: Addison-Wesley.
- WELSH, A.H. 1988. Asymptotically efficient estimation of the sparsity function at a point. *Statistics and Probability Letters*, **6**, 427–432.
- WITHERS, C.S., & NADARAJAH, S. 2010. Methods for symmetrizing random variables. *Probability in the Engineering and Informational Sciences*, **24**, 549–559.

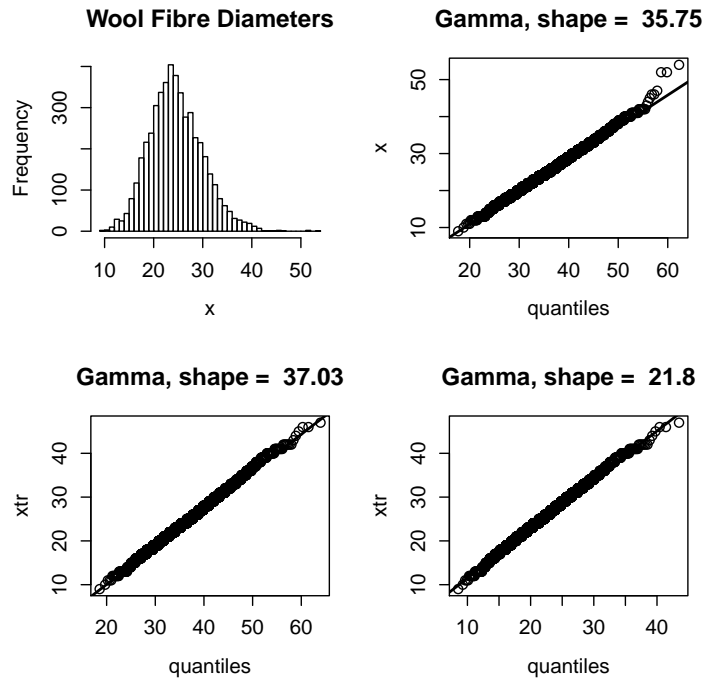


Figure 6: Histogram of wool fibre diameter data x and QQ-plots of fitted gamma model for these data and also for two fitted gamma models for truncated data xtr ; data and details of analysis are found in Section 7.1.

7 Appendix

7.1 Wool fibre diameter data

A histogram of wool fibre diameters is shown in the upper left hand plot of Figure 6; it is reproduced from (Botha & Hunter, 2010, p.246). The data can be loaded into R and a statistical summary obtained with the following commands: here $d = 9, 10, \dots, 54$ is a vector of diameters in microns, f is a vector of their frequencies and x is the sorted data, numbering $n = 4817$.

```
d <- c(seq(9,54))
f <- c(1,1,3,10,29,25,43,79,117,178,216,238,305,337,361,404,378,336,277,288,227)
f <- c(f,215,181,139,113,79,62,48,31,27,22,19,12,7,1,1,1,2,1,0,0,0,0,2,0,1)
x <- rep.int(d,f)
summary(x)
```

Min.	1st Qu.	Median	Mean	3rd Qu.	Max.
9.00	21.00	25.00	25.08	28.00	54.00

The top right plot of Figure 6 shows a QQ plot of these data versus the quantiles of a Gamma distribution with shape parameter 35.75, the best fitting model of Table 6. Visually it is very similar to QQ-plots using the Gamma model and shape estimates with values ranging from 22 to 37. The QQ-plots for the best-fitting Weibull models in Table 6 are not shown because they are non-linear and so the Weibull models are unsuitable for fitting these data.

It was thought that the outliers 52, 52 and 54 might be affecting the fits of the Gamma models, so they were fitted again after omitting them; the truncated data is called 'xtr', and it has maximum 47, one sd less than the omitted values. In the bottom left-hand plot of Figure 6 it is seen that the QQ-plot for the best fitting Gamma model found by method H -pdQ, is almost linear, and similarly on its right for shape obtained by the MLE method.

7.2 Proof of Proposition 1

Part (a) is Theorem 2.2 of Withers & Nadarajah (2010). Part (b) is a straightforward modification of the proof of Part(a): let X have a distribution on the integers with $P(X = i) = p_i$ and let Y be a symmetric distribution on the integers with $P(Y = i) = q_i$, so $q_{-i} = q_i$, $i \geq 1$. Amongst such q we will minimize the divergence $I(p : q) = \sum_i p_i \ln(p_i/q_i) = \sum_i p_i \ln(p_i) - p_0 \ln(q_0) - \sum_{i=1}^{\infty} (p_i + p_{-i}) \ln(q_i)$. Taking λ as a Lagrange multiplier, we need to solve $0 \equiv \frac{\partial}{\partial q_i} \{I(p : q) + \lambda \sum_i q_i\}$. This yields $0 = -p_0/q_0 + \lambda$ and $0 = -(p_i + p_{-i})/q_i + 2\lambda$ for $i > 0$. Therefore $q_0 = p_0/\lambda$ and $q_i = (p_i + p_{-i})/(2\lambda)$. The condition $\sum_i q_i = 1$ then implies $\lambda = 1$. Thus $q_i = (p_i + p_{-i})/2$ for all i . Clearly this result can be extended to an arbitrary discrete distribution on a lattice of points $\mathcal{X} = \{x_i\}$ by extending \mathcal{X} to $\mathcal{X} \cup -\mathcal{X}$, letting $P(X = x_i) = p_i$ and using the same argument. The absolutely continuous case then follows by approximating the density over a lattice with smaller and smaller increments and taking the limit.

For part (c), again return to a given discrete distribution p on the integers, and a symmetric distribution q on the integers. For each positive integer i introduce $2a_i = \ln(p_i p_{-i})$ and $\nu_i = \sqrt{p_i p_{-i}} = \exp(a_i)$. Further let $\bar{p}_i = (p_i + p_{-i})/2$. To minimize the KLD between p and q by choice of symmetric q we need to minimize

$$J(p, q) = \sum_i p_i \ln(p_i) - p_0 \ln(q_0) - 2 \sum_{i=1}^{\infty} \bar{p}_i \ln(q_i) + q_0 \ln(q_0/p_0) + 2 \sum_{i=1}^{\infty} q_i (\ln(q_i) - a_i) .$$

Setting the derivatives $0 \equiv \frac{\partial}{\partial q_i} \{J(p, q) + \lambda \sum_i q_i\}$ yields $0 = -p_0/q_0 + \ln(q_0/p_0) + 1 + \lambda$ and $0 = 2\{-\bar{p}_i/q_i + \ln(q_i) - a_i + 1 + \lambda\}$ for $i > 0$. The solution for q is implicit in:

$$\begin{aligned} q_0 &= p_0 \exp\{p_0/q_0\} e^{-\lambda-1} ; \\ q_i &= \nu_i \exp\{\bar{p}_i/q_i\} e^{-\lambda-1} , \text{ for } i \geq 1 ; \\ 1 &= q_0 + 2 \sum_{i=1}^{\infty} q_i . \end{aligned} \tag{7}$$

As in parts (a) and (b), the proof of part (c) is completed by a limiting argument.

Algorithm for computing the solution to (7). Given a discrete distribution p , \mathcal{X} , one may solve the equations (7) iteratively. For the continuous case we solved the equations (5) as follows:

1. Given f_1 compute $\nu(x) = \sqrt{f_1(x) f_1(-x)}$ and $\bar{f}_1(x) \equiv \{f_1(x) + f_1(-x)\}/2$.
2. Fix $C = e^{-\lambda-1} > 0$ and for each x in a fine grid over the support of f_1 solve for $\beta(x; C)$

$$\beta(x) = \nu(x) \exp\{\bar{f}_1(x)/\beta(x)\} C .$$

Numerically compute $d_C = \int \beta(x; C) dx$, normalize $\beta(x; C)$ to a probability density $f_2(x; C) = \beta(x; C)/d_C$ and use it to calculate $J(1, 2; C)$.

3. Repeat the last step for a range of C values to locate the $C = C_{opt}$ for which $J(1, 2; C)$ is minimized. This $f_2(x; C_{opt})$ is the solution guaranteed by (5).

Examples of computing (7). In the left plot of Figure 7 are shown the symmetric densities closest to the lognormal pdQ (in minimizing the divergences $I(1 : 2)$, $I(2 : 1)$ and $J(1, 2)$). Also shown are values $J(1, 2; C) = \int \{f_1(u) \log(f_1(u)/f_C(u)) + f_C(u) \log(f_C(u)/f_1(u))\} du$, where $f_C(u) \equiv f_2(x; C) = \beta(x; C)/d_C$ in the iterative Step 2 above. Figure 8 gives the corresponding results for the Pareto $a = 1$. An R script for creating Figure 8 is in the supplementary online material.

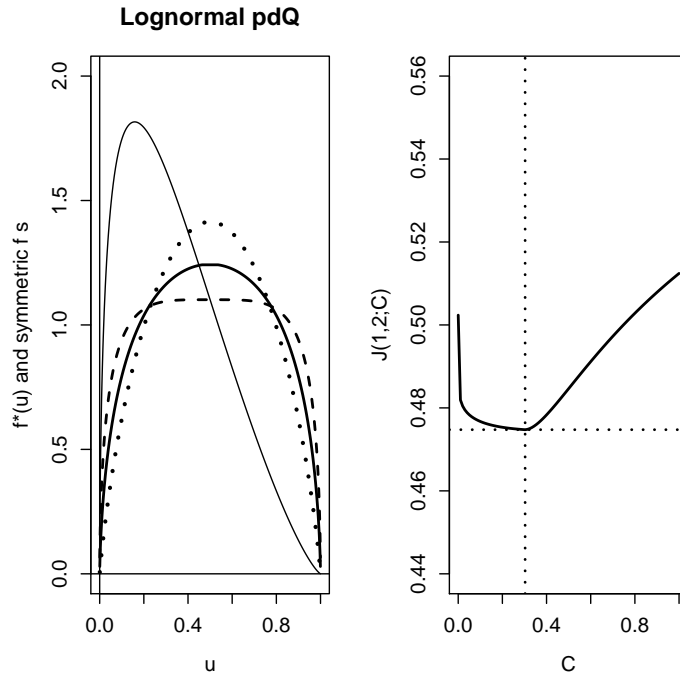


Figure 7: On the left is shown the lognormal pdQ $f^*(u)$ (thin solid line) and the respective closest symmetric densities on $[0,1]$ that minimize $I(1:2)$ (dashed line), $I(2:1)$ (dotted line) and $J(1,2)$ (thick solid line). On the right is shown the graph of $J(1,2;C)$ for various C ; the $C_{opt} = 0.303$ which minimizes the KLD distance $J(1,2)$ is marked by a vertical line. The closest symmetric density in the Hellinger metric to the lognormal pdQ is the same as that minimizing $J(1,2)$.

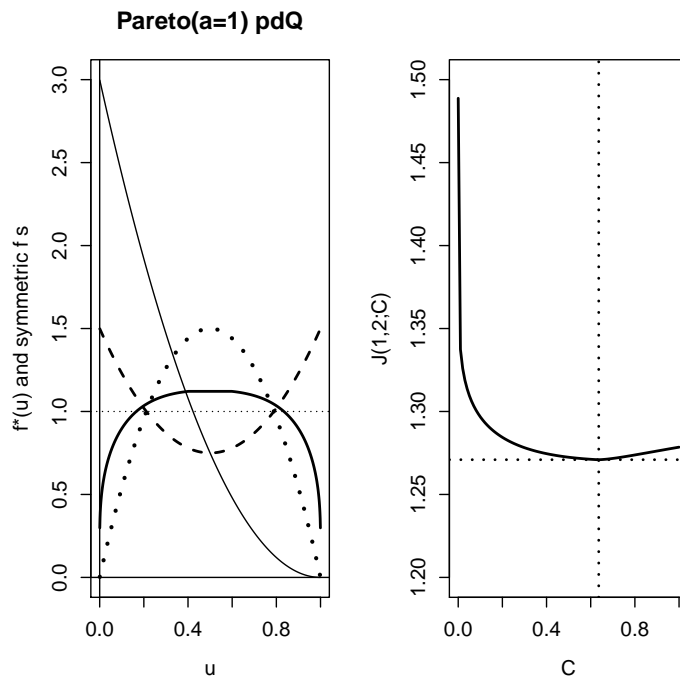


Figure 8: On the left is shown the Pareto($a = 1$) pdQ $f^*(u)$ (thin solid line) and the respective closest symmetric densities on $[0,1]$ that minimize $I(1:2)$ (dashed line), $I(2:1)$ (dotted line) and $J(1,2)$ (thick solid line). On the right is shown the graph of $J(1,2;C)$ for various C ; the $C_{opt} = 0.636$ which minimizes the KLD distance $J(1,2)$ is marked by a vertical line. The dotted horizontal line at 1 marks the uniform density, which is the closest symmetric density on $[0,1]$ in the Hellinger metric to this Pareto pdQ, and for this example it differs from the symmetric density minimizing $J(1,2)$.